ELSEVIER

Chemical Engineering Journal 78 (2000) 21–28

Chemical Engineering Journal

www.elsevier.com/locate/cej

Phenomenological model for bubble column reactors: prediction of gas hold-ups and volumetric mass transfer coefficients

K. Shimizu, S. Takada, K. Minekawa, Y. Kawase*

Biochemical Engineering Research Center, Department of Applied Chemistry, Toyo University, Kawagoe, Saitama 350-8585, Japan

Received 25 April 1999; received in revised form 8 October 1999; accepted 22 October 1999

Abstract

Based on a phenomenological model for bubble break-up and coalescence, a new simulation model for gas hold-up and gas-liquid mass transfer in bubble column reactors is proposed. In order to describe bubble movements in a bubble column reactor, a compartment concept is combined with the phenomenological model for bubble break-up and coalescence. It is assumed that the bubble column reactor consist of a series of discrete compartments in which bubble break-up and coalescence occur and bubbles move from compartment to compartment with different velocities. Gas hold-up and gas-liquid mass transfer rate are evaluated on the basis of bubble behaviors, i.e., bubble break-up and coalescence. Reasonable agreement is found between the model predictions and the present experimental data obtained in two different size bubble column reactors with air–water system and available correlations in the literature. Simulation results indicate that the proposed model provides some insight into the transport phenomena in bubble column reactors and furthermore it is useful for improving CFD predicting gas hold-ups and gas-liquid mass transfer rates in bubble column reactors.

Keywords: Bubble column reactor; Bubble break-up; Bubble coalescence; Gas hold-up; Volumetric mass transfer coefficient

1. Introduction

Bubble column reactors have been widely adopted in the chemical and biochemical industries. However, the design and scale-up of bubble column reactors are still very difficult and their approaches are largely empirical [1,2]. Although a number of empirical correlations have been used for bubble column reactor design, they can shed little light on the mechanism of physical processes occurring in bubble column reactors. In bubble column reactors, the size of bubbles is the most important parameter deciding their performance. It determines the bubble rising velocity and the gas residence time and governs the gas hold-up, the interfacial area and as a result gas–liquid mass transfer rate. In gas–liquid two-phase systems, bubble break-up and coalescence can profoundly influence the overall performance, by altering the interfacial area available for mass transfer between the phases. Therefore, it is essential to understand the bubble behavior for rational design of bubble column reactors and there have been extensive studies related to this aspect [2]. It is expected to obtain some insight into the phenomena in bubble column reactors through simulation models based on the mechanism of bubble phenomena, i.e., bubble break-up and coalescence.

Recently numerical simulation has been recognized as an ultimate tool for scale-up and design of chemical reactors and several studies have been conducted to understand hydrodynamics in bubble column reactors using computational fluid dynamic (CFD) models [3–5]. In the numerical simulations proposed for hydrodynamics in bubble column reactors, bubble phenomena have not been sufficiently taken into account [4]. In order to provide comprehensive pictures of bubble phenomena in bubble column reactors, therefore, an establishment of simulation model based on bubble break-up and coalescence phenomena is required.

Population balance models have been successfully used to describe liquid–liquid dispersion properties [6–9]. An advantage of the population balance approach is that the details of the break-up and coalescence processes can be included. Bapat et al. [10] and Ribeiro et al. [11] employed a population balance approach to predict the dispersed phase drop size distribution and mass transfer in liquid–liquid dispersion systems. Unfortunately, few studies have focused on gas–liquid systems and the understanding of gas dispersion in liquids is poor. Mihail and Straja [12] discussed bubble size distributions in bubble columns by applying a population balance concept. They did not examine the influence of bubble size distributions on the overall performance of bubble columns, such as gas hold-up and mass transfer. Prince and Blanch [13] proposed a phenomenological

* Corresponding author. Tel.: +81-492-39-1377; fax: +81-492-31-1031.
E-mail address: bckawase@eng.toyo.ac.jp (Y. Kawase)

1385-8947/00/$ – see front matter
PII: S1385-8947(99)00165-5

model for the rates of bubble break-up and coalescence in turbulent gas–liquid dispersions. They compared the model and the experimental data for the rates of bubble break-up and coalescence and for the average bubble size and bubble size distribution. They found good agreement between the model predictions and the experimental data. This implies that the proposed model for the rates of bubble coalescence and bubble break-up in gas–liquid dispersions is reasonable. However, their model was not applied to predict important design parameters for bubble column reactors such as gas hold-ups and gas–liquid mass transfer rates. In this study, we modify and extend their approach to discuss the overall performance of a bubble column reactor. Utilizing the bubble population balance model coupled with appropriate models of break-up and coalescence functions and the compartment model for bubble movements in a bubble column reactor, gas hold-ups and gas–liquid volumetric mass transfer rates are analyzed. In the proposed model, the bubble column is assumed to consist of a series of discrete compartments in which bubble break-up and coalescence occur. Bubbles are considered to move from compartment to compartment with different velocities. The capability of the model is examined using the present experimental results obtained in two different size bubble columns and available correlations in the literature.

2. Model development

2.1. Bubble break-up and coalescence

Bubble size depends on a balance of coalescence and break-up rates in the bubble column reactor. In the simulation, the bubble behavior is considered by simply observing the bubbles one by one. We develop a model for bubble behavior on the basis of the phenomenological model for the rates of bubble break-up and coalescence used by Prince and Blanch [13]. Their approach is based on the phenomenological model for liquid–liquid dispersions proposed by Coulaloglou and Tavlarides [7].

2.1.1. Bubble break-up

Bubble break-up is modeled by a two-step mechanism; the deformation of a bubble due to interactions with the turbulent flow field and the break-up of the deformed bubbles.

The break-up rate of bubbles in a turbulent flow is given by the product of the eddy-bubble collision frequency and the break-up efficiency. In this work, for lack of adequate theoretical and experimental knowledge, it is assumed that a bubble breaks into two equal size daughter bubbles [9,14].

The resulting equation for the total break-up rate of all bubbles, β_T, may be given as [9,13]:

$$\beta_T = \sum_i \sum_e F(u)\theta_{ie} \tag{1}$$

The total break-up rate of all bubbles can be estimated by taking account of all possible pairings of bubbles and turbulent eddies. The range of turbulent eddy sizes, which must be considered, is from the Kolmogoroff scale to the bubble size [9]. The turbulent collision rate, θ_{ie}, for a bubble of diameter, d_{bi}, with an eddy of diameter, d_e, is

$$\theta_{ie} = n_i n_e S_{ie}(u_{ti}^2 + u_{te}^2)^{1/2} \tag{2}$$

The velocities of a bubble having diameters of d_{bi} and an eddy having diameters of d_e, u_{ti} and u_{te}, may be written as [14–16]

$$u_{ti} = 1.4\varepsilon^{1/3} d_{bi}^{1/3} \tag{3}$$

and

$$u_{te} = 1.4\varepsilon^{1/3} d_e^{1/3} \tag{4}$$

respectively. The eddy diameter, d_e, may be evaluated using Kolmogoroff's theory of isotropic turbulence [17,18].

$$d_e = \left(\frac{\nu_l^3}{\varepsilon}\right)^{1/4} \tag{5}$$

where ν_l is the kinematic viscosity of the liquid phase. An energy dissipation rate, ε, in a bubble column reactor is written as [1]:

$$\varepsilon = U_g g \tag{6}$$

Here g is the gravitational acceleration. The collision cross-section area, S_{ie}, in Eq. (2) may be written as:

$$S_{ie} = \frac{\pi}{4}(d_{bi} + d_e)^2 \tag{7}$$

The number of eddies per unit mass of the fluid, n_e, in Eq. (2) is evaluated by the following relationship derived by Azbel [19]

$$\frac{dn_e(k)}{dk} = 0.1\frac{k^2}{\rho_l} \tag{8}$$

The eddy wave number, k, is defined as an inverse of the radius of the eddy, $d_e/2$. Integration of Eq. (8) yields the number of eddies.

The fraction of eddies having sufficient energy to cause rupture, $F(u)$, in Eq. (1) is given by [7]:

$$F(u) = \exp\left\{-\left(\frac{u_{ci}^2}{u_{te}^2}\right)\right\} \tag{9}$$

in which u_{ci} is the critical eddy velocity for break-up of a bubble of diameter d_{bi} and may be written as:

$$u_{ci} = \left(\frac{\sigma}{d_{bi}\rho_l}\right)^{1/2} \tag{10}$$

where σ is the surface tension and ρ_l is the density of the liquid phase. Prince and Blanch [13] used a relationship

for u_{ci} based on the expression for the maximum stable bubble size derived by Bhavaraju et al. [20]. Instead of their somewhat indistinct relationship, Eq. (10) is used [21]. Using the above equations, the total break-up rate for bubbles, β_T, can be estimated.

2.1.2. Bubble coalescence

In a turbulent flow field, the bubbles first collide and then remain in contact for sufficient time so that the processes of film drainage, film rupture and coalescence occurs. The coalescence rate is written as the product of a collision rate and a coalescence efficiency or probability.

It is assumed that bubble collisions occur due to turbulent fluctuation of liquid phase, buoyancy forces of bubbles and shear stresses of liquid phase [13]. The overall coalescence rate, χ_T, is given by

$$\chi_T = \frac{1}{2}\sum_i\sum_j \left\{\lambda_{ij}(\theta_{ij}^T + \theta_{ij}^B + \theta_{ij}^S)\right\} \tag{11}$$

The overall coalescence rate is obtained by considering all possible pairings of the bubbles. The turbulent collision rate, θ_{ij}^T, for two bubbles of diameter d_{bi} and d_{bj} is given as a function of bubble size, concentration and velocity:

$$\theta_{ij}^T = n_i n_j S_{ij}(u_{ti}^2 + u_{tj}^2)^{1/2} \tag{12}$$

Here, n_i and n_j are the concentrations of bubbles of diameter d_{bi} and d_{bj}, respectively.

The buoyant collision rate, θ_{ij}^B, is

$$\theta_{ij}^B = n_i n_j S_{ij}(u_{ri} - u_{rj}) \tag{13}$$

The rising velocity of the bubble in the turbulent flow regime u_{ri} in Eq. (13) can be evaluated by [5]

$$u_{ri} = \left(2.14\frac{\sigma}{\rho_l d_{bi}} + 0.505 g d_{bi}\right)^{1/2} \tag{14}$$

The collision rate due to shear, θ_{ij}^S, is given as [13]:

$$\theta_{ij}^S = n_i n_j \frac{4}{3}\left(\frac{d_{bi}}{2} + \frac{d_{bj}}{2}\right)^3 \left(\frac{dU_l}{dr}\right) \tag{15}$$

The shear rate for the shear stress exerted on the bubble, (dU_l/dr), is postulated to be characterized as:

$$\frac{dU_l}{dr} \approx \frac{U_l}{D_T/2} = \frac{0.787(gD_T U_g)^{1/3}}{D_T/2} \tag{16}$$

The liquid recirculation induced due to radial distribution of gas hold-up can be observed in a bubble column reactor. Kawase and Moo-Young [22] analyzed the liquid phase mixing using an energy balance and the mixing length theory. As the characteristic liquid velocity, U_l, in a bubble column having diameter of D_T at superficial gas velocity of U_g in Eq. (16), the liquid velocity at the column axis derived by Kawase and Moo-Young [22] is applied.

The collision efficiency for bubble coalescence, λ_{ij}, in Eq. (11) is

$$\lambda_{ij} = \exp\left(-\frac{t_{ij}}{\tau_{ij}}\right) \tag{17}$$

where τ_{ij} is the contact time for the two bubbles and given by [23]

$$\tau_{ij} = \frac{(d_{ij}/2)^{2/3}}{\varepsilon^{1/3}} \tag{18}$$

The time required for coalescence of two bubbles having diameter d_{bi} and d_{bj}, t_{ij}, is estimated to be the time required to film drainage between the bubbles.

$$t_{ij} = \left\{\frac{(d_{ij}/2)^3 \rho_l}{16\sigma}\right\}^{1/2} \ln\left(\frac{h_0}{h_f}\right) \tag{19}$$

The equivalent radius for bubble coalescence, d_{ij}, is [24]

$$d_{ij} = \left(\frac{2}{d_{bi}} + \frac{2}{d_{bj}}\right)^{-1} \tag{20}$$

Here, h_0 is the initial film thickness with h_f which is the critical film thickness at which rupture occurs. This relationship for bubble–bubble coalescence was derived by Kirkpatrick and Lockett [25]. As well as the work of Prince and Blanch [13], the initial and final film thickness in air-water systems are assumed to be 1×10^{-4} and 1×10^{-8} m, respectively. The equations given above are used to estimate bubble coalescence rates, β_T.

2.2. Gas hold-up

The size distribution is obtained as a result of bubble break-up and coalescence occurring simultaneously in the hypothetical compartment. Adding simply the volume of all bubbles, V_{bi}, and dividing by the dispersion volume, V_R, consisting of the total volume of gas, V_g, and that of liquid, V_l, the gas hold-ups, ϕ, can be calculated.

$$\phi = \frac{V_g}{V_g + V_l} = \frac{\sum_i V_{bi}}{V_R} \tag{21}$$

2.3. Volumetric mass transfer coefficient

The specific surface area, a, is related to gas hold-up by the following equation [1,26].

$$a = \frac{6\phi}{d_{VS}} \tag{22}$$

where d_{VS} is the Sauter mean diameter which is a measure of the interfacial area per unit volume of the gas phase.

The Higbie penetration theory [1,26] gives the following relationship for liquid-phase mass transfer coefficient k_L:

$$k_L = \left(\frac{4D_L u_r}{\pi d_b}\right)^{1/2} \tag{23}$$

where D_L is diffusivity. Combining Eqs. (22) and (23) yields the expression for $k_L a$ in a bubble column reactor

$$k_L a = \sum_i \left(\frac{4 D_L u_{ri}}{\pi d_{bi}}\right)^{1/2} \left(\frac{6\phi_i}{d_{bi}}\right) \tag{24}$$

During the repeated break-up and coalescence of bubbles, hydrodynamics in the vicinity of a gas–liquid surface may affect mass transfer rate. However, its effects in turbulent flows are still not quantitatively described or even fully understood. In this study, therefore, no influence of break-up and coalescence of bubbles and of interactions among adjacent bubbles on mass transfer is assumed as well as the works for liquid–liquid dispersions of Bapat et al. [10] and Ribeiro et al. [11].

2.4. Simulation procedure

A bubble column is assumed to be separated into hypothetical compartments being completely mixed stage. The schematic flow diagram is illustrated in Fig. 1. The volume of the bubble column reactor having height of H_L is divided into a series of M discrete compartments, each having a same height ΔH ($=H_L/M$). In a compartment bubble break-up and coalescence occur simultaneously and the bubble size distribution changes. The compartment height ΔH or the number of compartments M is somewhat arbitrary but it must be larger than the maximum bubble size and smaller than the distance of bubble rising. The typical value of M in this study was 500. The time is divided into segments of Δt. This time segment is also somewhat arbitrary but it must be larger than the time required for bubble break-up and coalescence. If it is too large, the accuracy of the calculation is poor. In this study, we used a fixed time increment for an occurrence of an event. The typical time increment used in this study was 0.05 s. The number of compartment and time increment were selected by varying them to ensure that the results were independent of them. An event, if it occurs, is assumed to occur at the beginning of the time increment and only one break-up or coalescence is allowed in one observation time Δt [10].

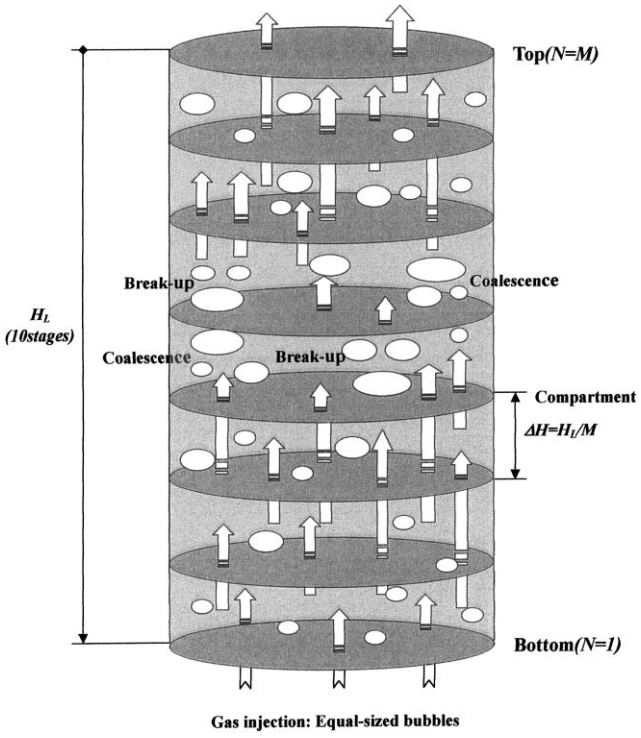

Fig. 1. Schematic flow diagram of the compartment model.

Bubbles move from lower compartment to upper compartment according to bubble rising velocity. When a gas is sparged into a bubble column reactor, the gas fraction is higher at the center of the reactor than at the wall. As described above, the resulting radial density gradient induces a buoyancy-driven liquid circulation, with upflow in the core and downflow in the outer annulus [27]. Bubbles of different sizes travel at different velocities represented by Eq. (14). It is assumed, therefore, that the actual rising motion of bubbles, u'_r, can be represented by the following relationship:

$$u'_r = u_r + cU_l \tag{25}$$

where u_r is a bubble velocity in a still liquid estimated using Eq. (14). The second term in the RHS of Eq. (25) is introduced to consider the influence of liquid recirculation on bubble rising velocity. The proportionality constant c in Eq. (25) was temporarily assumed to be 2/3. This constant is introduced to replace liquid circulations with characteristic liquid upflows. More discussion for this simplification is required.

The number of compartments ΔN which the bubble moves during Δt is given by

$$\Delta N = \left(u'_r \frac{\Delta t}{\Delta H}\right) \tag{26}$$

ΔN is integer by raising fractions to unit. Consequently, a new compartment of the bubble $N_{t+\Delta t}$ can be obtained as:

$$N_{t+\Delta t} = N_t + \Delta N \tag{27}$$

Gas is injected to the bottom compartment. It is assumed that equal-sized bubbles are continuously injected to the bottom of the bubble column reactor or the first compartment (N=1). The incoming gas phase is assumed to consist of uniform size of bubbles and the number of bubbles formed by the sparger at the reactor bottom is determined from the gas flow rate and the initial bubble size.

At the start of a simulation, bubbles having a uniform size exist only in the bottom compartment. From the bottom compartment to top compartment, the new bubble size distribution is calculated by taking account of the rates for bubble break-up and coalescence calculated by Eqs. (1) and (11) and then their new locations are evaluated from their rising velocities using Eq. (27). The same simulation procedure for a number of simulation times is repeated. The

scale of eddies effective to bubble break-up is ranged from the smallest possible eddy, $d_{e\min}$, to the largest eddy, $d_{e\max}$. The smallest eddy is estimated using Eq. (5) multiplied by 2 [13] and the largest eddy is equal to bubble size [9,28]. Therefore, the eddy size intervals used to calculate the bubble break-up rate is $(d_{e\max}-d_{e\min})/100$ m. The bubble size interval between the minimum bubble size of 0.001 m and the maximum bubble size of 0.015 m is 0.0005 or 0.001 m. In other words, the number of bubble size intervals used was 15 or 30 in the present simulations.

It is postulated for simplicity that bubbles cannot go back into the lower compartments. In other words, only forward movements of bubbles are considered. The effects of the presence of liquid backflow accompanying small bubbles on gas hold-up and volumetric mass transfer coefficient is taken into account by introducing the characteristic liquid flow rate. In bubble column reactors, an upward liquid flow is observed in the center portion and a downward liquid flow near the reactor wall. Some small bubbles are dragged by the downward liquid flow [2,22]. The effects of liquid backflow and radial distribution of axial liquid velocity on bubble movement are approximately considered using the characteristic liquid velocity evaluated by introducing the proportionality constant c into Eq. (25) instead of the direct use of the actual or local liquid velocity.

The simulation runs are continued till the steady state is attained. The steady-state solution can be obtained when the change in gas hold-up becomes negligible. Under this condition, bubble break-up and coalescence are in balance and the gas hold-up is therefore time-independent. Several simulation passes are required before a steady-state solution can be obtained. After steady state had been attained, we determined gas hold-ups and volumetric mass transfer coefficients through the bubble column.

3. Experimental

Experiments were carried out in a column 0.20 m in diameter and 1.7 m in height and a bubble column 0.155 m in diameter and 0.834 m in height. A ring sparger with 12 holes of 1.0 mm diameter was used in the 0.20 m i.d. column. Perforated plates 57 holes of 1.0 mm diameter and 89 holes of 1 mm diameter were used in the 0.155 m i.d. column. Tap water and air were used as the liquid phase and gas phase, respectively. The density, viscosity and surface tension of water were measured with a pycnometer, a Cannon–Fenske viscometer and the du-Nouy ring method, respectively. The operation was batchwise with respect to liquid phase. The rate of air-flow sparged continuously was measured with a precalibrated rotameter. The gas hold-ups were obtained by the volume expansion method. The volumetric mass transfer coefficients were determined by the dynamic method. The change in the dissolved oxygen concentration was monitored using a fast response dissolved oxygen electrode (YSI model 57, Yellow Springs Instrument Co.).

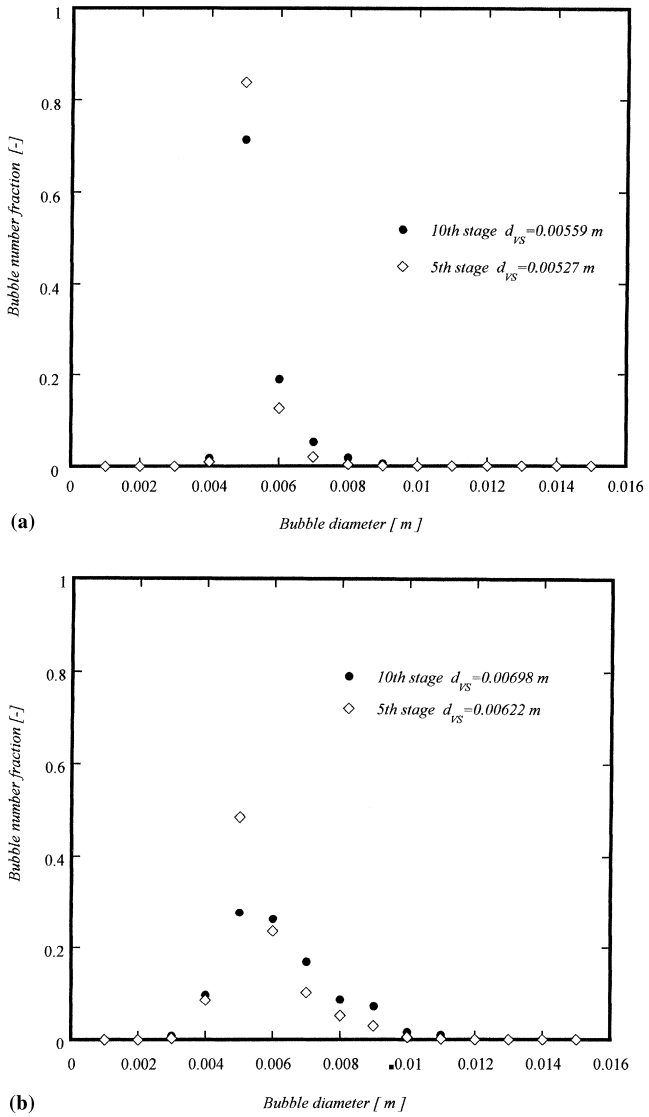

Fig. 2. (a) Simulated bubble size histogram in the 0.20 m i.d. bubble column reactor at U_g=0.01 ms^{-1}. (b) Simulated bubble size histogram in the 0.20 m i.d. bubble column reactor at U_g=0.04 ms^{-1}.

4. Results and discussion

4.1. Bubble size distribution

Simulation results for bubble size distributions in the 0.20 m i.d. bubble column reactor are shown in Fig. 2a and b. The bubble size distributions are results of bubble break-up and coalescence occurring simultaneously. In illustrating the simulation results, the bubble column is redivided to 10 stages. In the figures the Sauter mean diameters calculated from the proposed model are given. It is seen from the data for U_g=0.01 m s^{-1} in Fig. 2a that at the middle of the column (5th stage) the somewhat steep increase and decrease in number density can be obtained for smaller and larger bubbles, respectively, as compared with the top of the column (10th

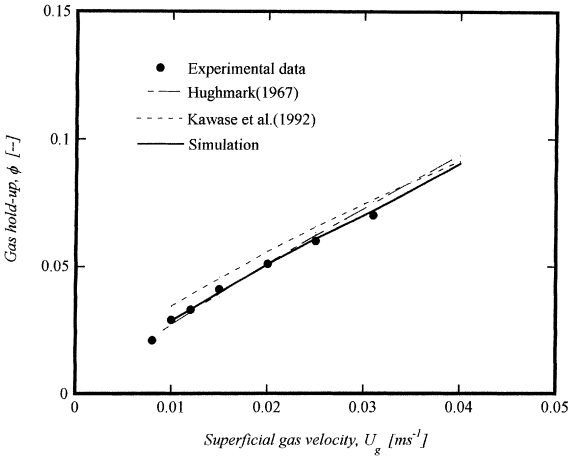

Fig. 3. Gas hold-ups in the 0.2 m i.d. bubble column reactor.

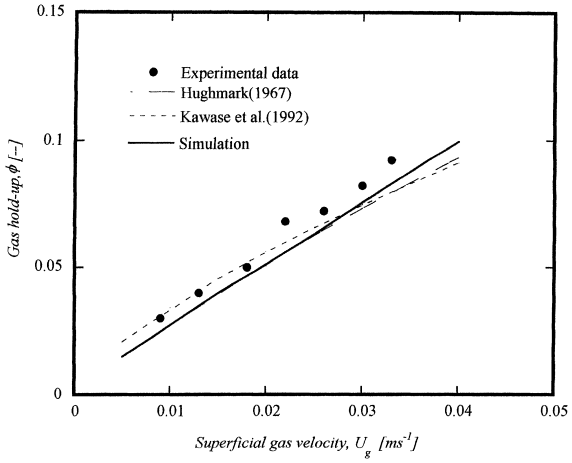

Fig. 4. Gas hold-ups in the 0.155 m i.d. bubble column reactor.

stage). This trend can be seen more clearly from the data for U_g=0.04 m s^{-1} in Fig. 2b. The feature of these data sets in shown Fig. 2a and b is that with increasing gas flow rate the peak in the number density shifts to the right and the bubble size distribution become lower and wider. At higher gas flow rates bubble break-up and coalescence more frequently occur as compared with those at lower gas flow rates and as a result the bubble size distribution becomes wider. The Sauter mean diameter at the top of the column somewhat increases with gas flow rate as well as the results of Jamialahmadi and Muller-Steinhagen [29]. This may be attributed to the enhancement of bubble coalescence along the column axis.

4.2. Gas hold-up

It is seen from Fig. 3 that the gas hold-ups in the 0.20 m i.d. bubble column are in agreement with the values predicted from the proposed simulation.

Hughmark [30] proposed an empirical correlation for gas hold-up. It may be written as:

$$\phi = \frac{1}{2 + (0.35/U_g)(\rho_l \sigma/72)^{1/3}} \quad (28)$$

The following theoretical correlation was derived by Kawase et al. [31].

$$\frac{\phi}{1-\phi} = 0.0625 \left(\frac{U_g^3}{\nu_l g}\right)^{1/4} \quad (29)$$

For reference, the predictions of Eqs. (28) and (29) are also shown in Fig. 3. They agree well with the present experimental data and the proposed simulation model.

In Fig. 4, the simulation model is compared with the experimental data in the 0.155 m i.d. bubble columns besides the predictions of Eqs. (28) and (29). The proposed simulation model can fit the data reasonably. It is also seen that the agreement between the model predictions and the predictions of Eqs. (28) and (29) is satisfactory.

Fig. 5 shows axial distributions of gas hold-up in the 0.20 m i.d. bubble column predicted by the proposed model. It can be seen that gas hold-up distributions are almost uniform at low and high gas flow rates.

4.3. Gas–liquid mass transfer

Fig. 6 depicts that the simulation model predictions are fairly close to the experimental data for $k_L a$ in the 0.2 m i.d. bubble column reactor.

An empirical correlation for gas–liquid volumetric mass transfer coefficient was developed by Akita and Yoshida [32].

$$\frac{k_L a D_T^2}{D_L} = 0.6 \left(\frac{\nu_l}{D_L}\right)^{0.5} \left(\frac{g D_T^2 \rho_l}{\sigma}\right)^{0.62} \left(\frac{g D_T^3}{\nu_l^2}\right)^{0.31} \phi^{1.1} \quad (30)$$

Shah et al. [1] obtained a simple correlation for $k_L a$ in a bubble column with air–water system which may be written as

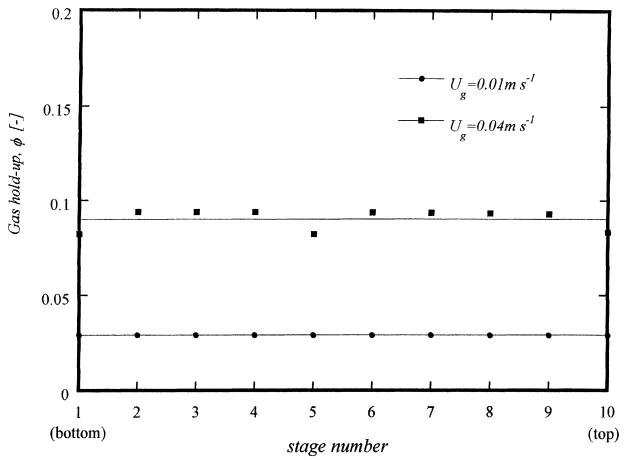

Fig. 5. Axial distribution of gas hold-up in a bubble column reactor (D_T=0.20 m).

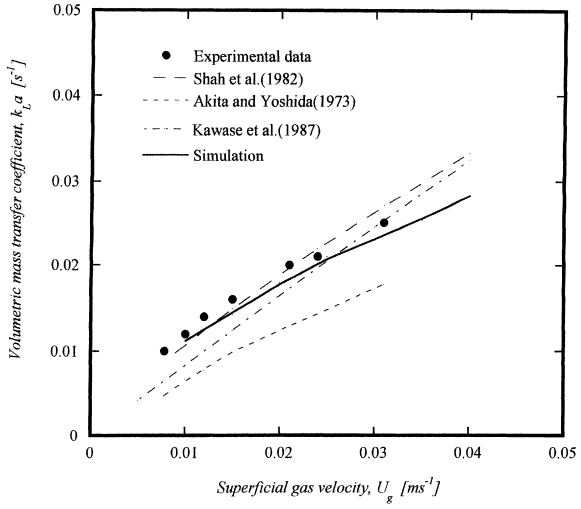

Fig. 6. Gas–liquid mass transfer rates in the 0.2 m i.d. bubble column reactor.

$$k_{\mathrm{L}}a = 0.467U_{\mathrm{g}}^{0.82} \tag{31}$$

Kawase et al. [33] proposed a semi-theoretical correlation for $k_{\mathrm{L}}a$ in a bubble column. Their correlation for Newtonian fluids is written as:

$$\frac{k_{\mathrm{L}}aD_{\mathrm{T}}^2}{D_{\mathrm{L}}} = 0.452\left(\frac{\nu_{\mathrm{l}}}{D_{\mathrm{L}}}\right)^{1/2}\left(\frac{D_{\mathrm{T}}U_{\mathrm{g}}}{\nu}\right)^{3/4}\left(\frac{gD_{\mathrm{T}}^2\rho_{\mathrm{l}}}{\sigma}\right)^{3/5} \times\left(\frac{U_{\mathrm{g}}^2}{D_{\mathrm{T}}g}\right)^{7/60} \tag{32}$$

For reference, the above correlations are given in Fig. 6. Eq. (30) predicts rather smaller $k_{\mathrm{L}}a$ values as compared with the experimental data. The predictions of the proposed simulation model and Eqs. (31) and (32) fit the data reasonably well.

Fig. 7 compares the predictions of the proposed simulation model with the experimental data in the 0.155 m i.d. bubble column. It can be seen that the proposed model agrees reasonably with the experimental data. The predictions of Eqs. (31) and (32) lie somewhat below the experimental data. It is also seen from Fig. 7 that Eq. (30) underestimates the $k_{\mathrm{L}}a$ coefficients in the 0.155 m i.d. bubble column.

In bubble column reactors, there are three flow regimes depending on reactor diameter and gas flow rates, bubbly flow, churn turbulent flow and slug flow. The hydrodynamics and heat and mass transfer depend strongly on the flow regime. As well as the study of Prince and Blanch [13], the proposed simulation model may be applicable to bubbly flow and churn turbulent flow regimes which are observed in the 0.155 and 0.20 m i.d. bubble columns. Additional examinations are in progress to clarify the flow conditions in which the proposed model is applicable.

In Fig. 8, axial distributions of $k_{\mathrm{L}}a$ in the 0.20 m i.d. bubble column reactor are plotted. The distribution of $k_{\mathrm{L}}a$ is not uniform. Larger $k_{\mathrm{L}}a$ values are predicted near the sparger. This coincides with the data reported in the literature [1]. At the low gas flow rate of U_{g}=0.01 m s^{-1}, the $k_{\mathrm{L}}a$ coefficients slightly decrease from the bottom to the top of the bubble column reactor. In the high gas flow rate region, a decrease in $k_{\mathrm{L}}a$ is significant. An increase in the number of larger bubbles near the top of the bubble column shown in Fig. 2 is responsible for the significant decrease in $k_{\mathrm{L}}a$. It is seen from Figs. 5 and 8 that the gas–liquid mass transfer rate is more sensitive to the bubble behaviors than the gas hold-up.

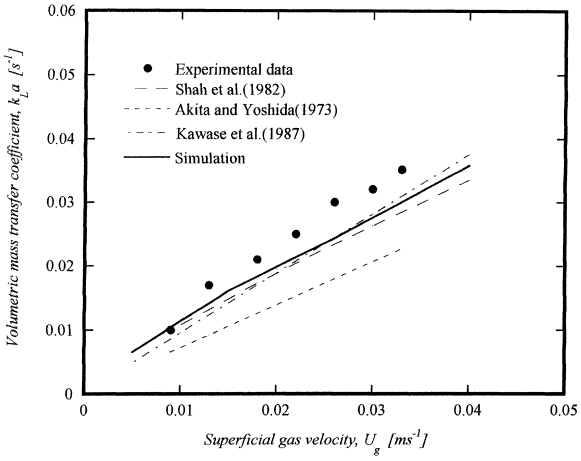

Fig. 7. Gas–liquid mass transfer rates in the 0.155 m i.d. bubble column reactor.

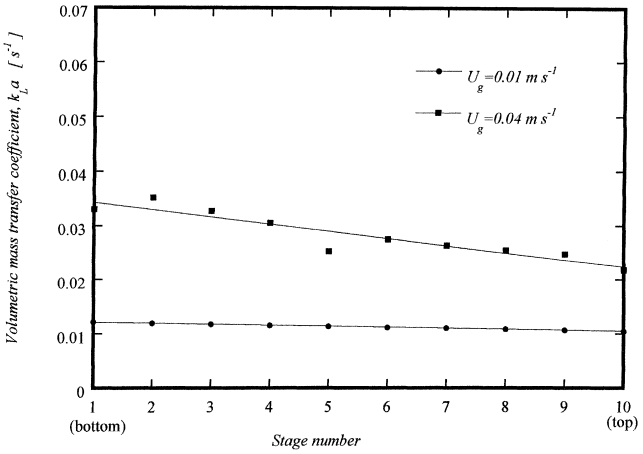

Fig. 8. Axial distribution of gas–liquid mass transfer rate in a bubble column reactor (D_{T}=0.20 m).

5. Conclusions

The simulation model based on the bubble behaviors in bubble columns has been developed. The bubble break-up and coalescence which are the primary phenomena in bubble column reactors are taken into account to evaluate gas

hold-ups and gas–liquid volumetric mass transfer rates. The present simulation is built on the phenomenological model for bubble break-up and coalescence proposed by Coulaloglou and Tavlarides [7] and Prince and Blanch [13]. The compartment model is applied to describe the bubble movements. Reasonable agreement between the simulation model and experimental results in the two different size bubble column reactors indicates that the model based on the physical picture for bubble dynamics could be used to predict bubble size distributions, gas hold-up and gas–liquid mass transfer rate. Due to the stochastic interaction of the bubble swarms some assumptions have been introduced. For instance, we assumed a binary bubble breakage. However, it is somewhat questionable that the two daughter bubbles have the same diameter. In this study, furthermore, the influence of liquid recirculation was treated only approximately. Although the proposed model cannot provide a complete description of bubble behaviors, it gives satisfactory insights of the phenomena in bubble column reactors. In order to improve the model, the effects of liquid recirculation in a bubble column reactor to bubble behaviors should be more precisely included. This study should be regarded as the first step to elucidate physical processes occurring in bubble column reactors through theoretical analyses based on the mechanism of bubble break-up and coalescence.

References

[1] Y.T. Shah, B.G. Kelkar, S.P. Godbole, W.D. Deckwer, AIChE J. 28 (1982) 353–379.
[2] W.D. Deckwer, Bubble Column Reactors, Wiley, New York, 1992.
[3] A. Lubbert, T. Paaschen, A. Lapin, Biotechnol. Bioeng. 52 (1996) 248–258.
[4] A. Sokolichin, G. Eigenberger, A. Lipin, A. Lubbert, Chem. Eng. Sci. 52 (1997) 611–626.
[5] T.-J. Lin, J. Reese, T. Hong, L.-S. Fan, AIChE J. 42 (1996) 301–319.
[6] K.J. Valentas, N.R. Amundson, Ind. Eng. Chem. Fundam. 5 (1966) 533–542.
[7] C.A. Coulaloglou, L.L. Tavlarides, Chem. Eng. Sci. 32 (1977) 1289–1297.
[8] M.A. Hsia, L.L. Tavlarides, Chem. Eng. J. 20 (1980) 225–236.
[9] C. Tsouris, L.L. Tavlarides, AIChE J. 40 (1994) 395–406.
[10] P.M. Bapat, L.L. Tavlarides, G.W. Smith, Chem. Eng. Sci. 38 (1983) 2003–2013.
[11] L.M. Ribeiro, P.F.R. Regueiras, M.M.L. Guimaraes, C.M.N. Madureira, J.J.C. Cruz-Pinto, Compters & Chem. Eng. 21 (1997) 543–558.
[12] R. Mihail, S. Straja, Chem. Eng. J. 33 (1986) 71–77.
[13] M.J. Prince, H.W. Blanch, AIChE J. 36 (1990) 1485–1499.
[14] G. Narsimhan, J.P. Gupta, D. Ramkrishna, Chem. Eng. Sci. 34 (1979) 257–265.
[15] J.C. Rotta, Turbulente Stromungen. B.G. Teubner, Stuttgart, 1972.
[16] R. Kuboi, I. Komasawa, T. Otake, J. Chem. Eng. Japan 5 (1972) 349–355.
[17] A. Kolmogoroff, C.R. (Doklady) Acad. Sci. USSR 30 (1941) 301–305.
[18] R.S. Cherry, E.T. Papoutsakis, Bioprocess Eng. 1 (1986) 29–41.
[19] D. Azbel, Two-Phase Flows in Chemical Engineering, Cambridge University Press, Cambridge, 1981.
[20] S.M. Bhavaraju, T.W.F. Russell, H.W. Blanch, AIChE J. 24 (1978) 454–466.
[21] M.A. Delichatsios, R.F. Probstein, Ind. Eng. Chem. Fundam. 15 (1976) 134–137.
[22] Y. Kawase, M. Moo-Young, Chem. Eng. Sci. 41 (1986) 1969–1977.
[23] V.G. Levich, Physicochemical Hydrodynamics, Prentice-Hall, Englewood cliffs, NJ, 1962.
[24] A.K. Chesters, G. Hofman, Appl. Sci. Res. 38 (1982) 353–361.
[25] R.D. Kirkpatrick, M.J. Lockett, Chem. Eng. Sci. 29 (1974) 2363–2373.
[26] K. Van't Riet, Trends in Biotechnology 1 (1983) 113–119.
[27] S.B. Kumar, N. Devanathan, D. Moslemian, M.P. Dudukovic, Chem. Eng. Sci. 49 (1994) 5637–5652.
[28] H. Luo, H.F. Svensen, AIChE J. 42 (1996) 1225–1233.
[29] M. Jamialahmadi, H. Muller-Steinhagen, Trans. I Chem. E. 68 (1990) 202–204.
[30] G.A. Hughmark, Ind. Eng. Chem. Process Des. Dev. 6 (1967) 218–220.
[31] Y. Kawase, S. Umeno, T. Kumagai, Chem. Eng. J. 50 (1992) 1–7.
[32] K. Akita, F. Yoshida, Ind. Eng. Chem. Process Des. Dev. 12 (1973) 76–80.
[33] Y. Kawase, B. Halard, M. Moo-Young, Chem. Eng. Sci. 42 (1987) 1609–1617.